



be used. Interactive views of meshes, fields and solid bodies are enabled by PyVista (Sullivan & Kaszynski, 2019). The capabilities of FElupe may be enhanced with additional Python packages, e.g. meshio (Schlömer, 2024), matadi (Dutzler, 2024b), tensortrax (Dutzler, 2024c), hyperelastic (Dutzler, 2024a) or feplot (Mohamed ZAARAOUI, 2023).

## Features

The essential high-level parts of solving problems with FElupe include a field, a solid body, boundary conditions and a job. A field for a field container is created by a mesh, a numeric region, see Figure 1.

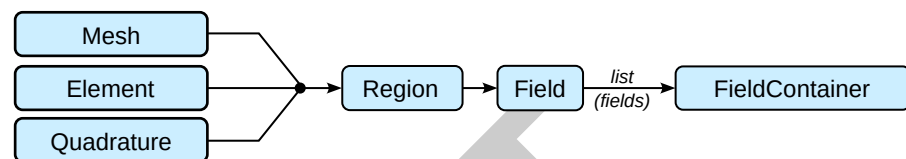


Figure 1: Schematic representation of classes needed to create a field container.

In a solid body, a constitutive material formulation is applied on this field container. Along with constant and ramped boundary conditions a step is created. During job evaluation, the field values are updated in-place after each completed substep as shown in Figure 2.

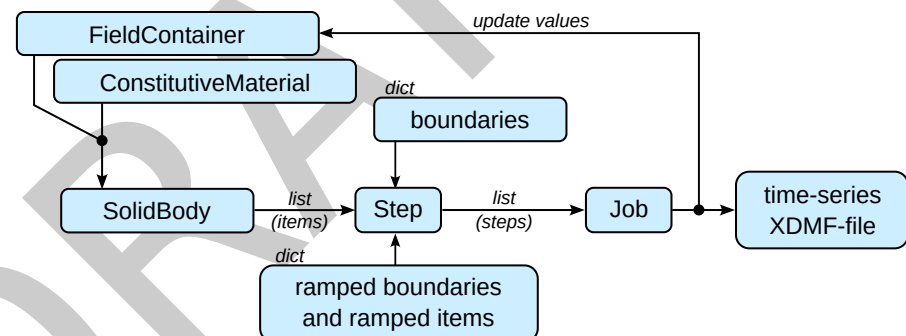


Figure 2: Schematic representation of classes needed to evaluate a job.

For example, consider a quarter model of a solid cube with hyperelastic material behavior subjected to a uniaxial elongation applied at a clamped end-face. First, a meshed cube out of hexahedron cells is created. A numeric region, pre-defined for hexahedrons, is created on the mesh. The appropriate finite element and its quadrature scheme are chosen automatically. A vector-valued displacement field is initiated on the region and is further added to a field container. A uniaxial load case is applied on the displacement field to create the boundary conditions. This involves setting up symmetry planes as well as the absolute value of the prescribed displacement at the mesh-points on the right-end face of the cube. The right-end face is clamped, i.e. its displacements, except the components in longitudinal direction, are fixed. An isotropic hyperelastic Neo-Hookean material formulation is applied on the displacement field of a solid body. A step generates the consecutive substep-movements of a selected boundary condition. The step is further added to a list of steps of a job. After the job evaluation is completed, the maximum principal values of logarithmic strain of the last completed substep are plotted, see Figure 3.

```
import felupe as fem
```

```
region = fem.RegionHexahedron(mesh=fem.Cube(n=6))
field = fem.FieldContainer([fem.Field(region, dim=3)])
solid = fem.SolidBody(umat=fem.NeoHookeCompressible(mu=1, lmbda=2), field=field)
boundaries, loadcase = fem.dof.uniaxial(field, clamped=True)

move = fem.math.linsteps([0, 1], num=5)
step = fem.Step([solid], ramp={boundaries["move"]: move}, boundaries=boundaries)
job = fem.Job(steps=[step]).evaluate()

solid.plot("Principal Values of Logarithmic Strain").show()
```

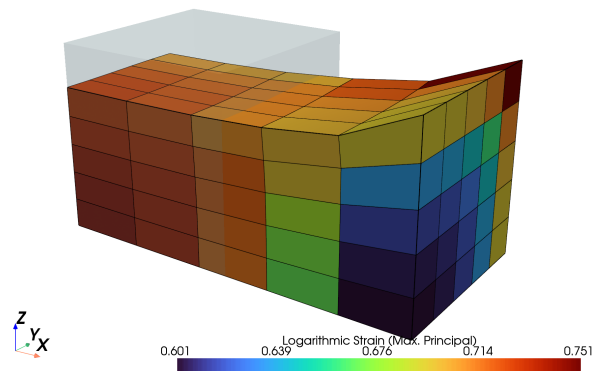


**Figure 3:** Final logarithmic strain distribution of the deformed hyperelastic solid body at  $l/L = 2$ . The undeformed configuration is shown in transparent grey.

Any other hyperelastic material model formulation may be used instead of the Neo-Hookean material model given above, most easily by its strain energy density function. The strain energy density function of the Mooney-Rivlin material model formulation, as given in Equation 1, is implemented by a hyperelastic material class in FElupe with the help of `tensortrax` (bundled with FElupe).

$$\psi(C) = C_{10} (\hat{I}_1 - 3) + C_{01} (\hat{I}_2 - 3) \quad (1)$$

```
import tensortrax.math as tm

def mooney_rivlin(C, C10, C01):
    I1 = tm.trace(C)
    I2 = (I1**2 - tm.trace(C @ C)) / 2
    I3 = tm.linalg.det(C)
    return C10 * (I3**(-1/3) * I1 - 3) + C01 * (I3**(-2/3) * I2 - 3)

umat = fem.Hyperelastic(mooney_rivlin, C10=0.5, C01=0.1)
solid = fem.SolidBody(umat=umat, field=field)
```

## Examples

The documentation of FElupe contains interactive tutorials and examples for simulating the deformation of solid bodies. Resulting deformed solid bodies of selected examples are shown in Figure 4. Computational results of FElupe are used in several scientific publications, e.g. (Dutzler et al., 2021), (Buzzi et al., 2022) and (Torggler et al., 2023).

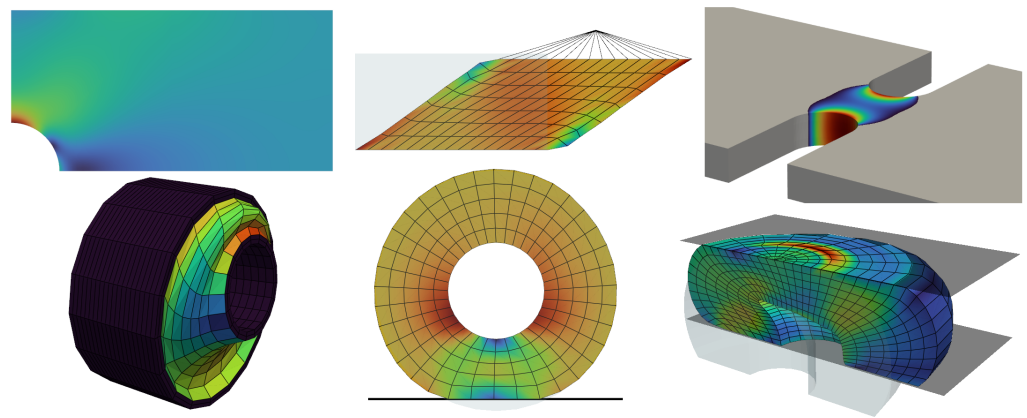


**Figure 4:** Equivalent stress distribution of a plate with a hole (top left). Shear-loaded hyperelastic block (top middle). Endurable cycles obtained by local stresses (top right). Multiaxially loaded rubber bushing (bottom left). Rotating rubber wheel on a frictionless contact (bottom middle). A hyperelastic solid with frictionless rigid contacts (bottom right).

## References

- 76
- 77 Ansel, J., Yang, E., He, H., Gimelshein, N., Jain, A., Voznesensky, M., Bao, B., Bell, P.,  
78 Berard, D., Burovski, E., Chauhan, G., Chourdia, A., Constable, W., Desmaison, A.,  
79 DeVito, Z., Ellison, E., Feng, W., Gong, J., Gschwind, M., ... Chintala, S. (2024). PyTorch  
80 2: Faster machine learning through dynamic python bytecode transformation and graph  
81 compilation. *Proceedings of the 29th ACM International Conference on Architectural  
82 Support for Programming Languages and Operating Systems, Volume 2*, 5, 929–947.  
83 <https://doi.org/10.1145/3620665.3640366>
- 84 Baratta, I. A., Dean, J. P., Dokken, J. S., Habera, M., Hale, J. S., Richardson, C. N.,  
85 Rognes, M. E., Scroggs, M. W., Sime, N., & Wells, G. N. (2023). *DOLFINx: The next  
86 generation FEniCS problem solving environment*. Zenodo. [https://doi.org/10.5281/zenodo.  
87 10447666%5D](https://doi.org/10.5281/zenodo.10447666%5D)
- 88 Bathe, K.-J. (2006). *Finite element procedures*. Bathe. ISBN: 9780979004902
- 89 Bonet, J., & Wood, R. D. (2008). *Nonlinear continuum mechanics for finite element analysis*.  
90 Cambridge University Press. <https://doi.org/10.1017/cbo9780511755446>
- 91 Bradbury, J., Frostig, R., Hawkins, P., Johnson, M. J., Leary, C., Maclaurin, D., Necula, G.,  
92 Paszke, A., VanderPlas, J., Wanderman-Milne, S., & Zhang, Q. (2018). *JAX: Composable  
93 transformations of Python+NumPy programs* (Version 0.3.13). [http://github.com/jax-ml/  
94 jax](http://github.com/jax-ml/jax)
- 95 Buzzi, C., Dutzler, A., Faethe, T., Lassacher, J., Leitner, M., & Weber, F.-J. (2022). Develop-  
96 ment of a tool for estimating the characteristic curves of rubber-metal parts. *Proceedings  
97 of the 12th International Conference on Railway Bogies and Running Gears*. ISBN: 978-  
98 963-9058-46-0
- 99 Cimrman, R., Lukeš, V., & Rohan, E. (2019). Multiscale finite element calculations in  
100 python using SfePy. *Advances in Computational Mathematics*, 45(4), 1897–1921. <https://doi.org/10.1007/s10444-019-09666-0>
- 102 Dutzler, A. (2024a). *Hyperelastic: Constitutive hyperelastic material formulations for FElupe*.  
103 Zenodo. <https://doi.org/10.5281/zenodo.8106469>
- 104 Dutzler, A. (2024b). *matADi: Material definition with automatic differentiation*. Zenodo.  
105 <https://doi.org/10.5281/zenodo.5519971>

- 106 Dutzler, A. (2024c). *Tensortrax: Math on (hyper-dual) tensors with trailing axes*. Zenodo.  
107 <https://doi.org/10.5281/zenodo.7384105>
- 108 Dutzler, A., Buzzi, C., & Leitner, M. (2021). Nondimensional translational characteristics  
109 of elastomer components. *Journal of Applied Engineering Design and Simulation*, 1(1).  
110 <https://doi.org/10.24191/jaeds.v1i1.20>
- 111 Gustafsson, T., & McBain, G. (2020). Scikit-fem: A python package for finite element assembly.  
112 *Journal of Open Source Software*, 5(52), 2369. <https://doi.org/10.21105/joss.02369>
- 113 Harris, C. R., Millman, K. J., Walt, S. J. van der, Gommers, R., Virtanen, P., Cournapeau, D.,  
114 Wieser, E., Taylor, J., Berg, S., Smith, N. J., Kern, R., Picus, M., Hoyer, S., Kerkwijk,  
115 M. H. van, Brett, M., Haldane, A., Río, J. F. del, Wiebe, M., Peterson, P., ... Oliphant,  
116 T. E. (2020). Array programming with NumPy. *Nature*, 585(7825), 357–362. <https://doi.org/10.1038/s41586-020-2649-2>
- 117
- 118 Mohamed ZAARAOUI. (2023). *ZAARAOUI999/feplot: v0.1.13*. Zenodo. <https://doi.org/10.5281/zenodo.10429691>
- 119
- 120 Renard, Y., & Poullos, K. (2020). *GetFEM: Automated FE modeling of multiphysics problems*  
121 *based on a generic weak form language*. <https://hal.science/hal-02532422>
- 122 Schlömer, N. (2024). *Meshio: Tools for mesh files*. Zenodo. <https://doi.org/10.5281/zenodo.1173115>
- 123
- 124 Sullivan, C., & Kaszynski, A. (2019). PyVista: 3D plotting and mesh analysis through a  
125 streamlined interface for the visualization toolkit (VTK). *Journal of Open Source Software*,  
126 4(37), 1450. <https://doi.org/10.21105/joss.01450>
- 127 Torggler, J., Dutzler, A., Oberdorfer, B., Faethe, T., Müller, H., Buzzi, C., & Leitner, M.  
128 (2023). Investigating damage mechanisms in cord-rubber composite air spring bellows  
129 of rail vehicles and representative specimen design. *Applied Composite Materials*, 30(6),  
130 1979–1999. <https://doi.org/10.1007/s10443-023-10157-1>
- 131 Xue, T., Liao, S., Gan, Z., Park, C., Xie, X., Liu, W. K., & Cao, J. (2023). JAX-FEM:  
132 A differentiable GPU-accelerated 3D finite element solver for automatic inverse design  
133 and mechanistic data science. *Computer Physics Communications*, 291, 108802. <https://doi.org/10.1016/j.cpc.2023.108802>
- 134
- 135 Zienkiewicz, O. C. (2013). *Finite element method: Its basis and fundamentals* (R. L.  
136 Taylor, J. Zhu, & O. C. Zienkiewicz, Eds.; 7th ed.). Elsevier Science & Technology.  
137 ISBN: 9780080951355